Stability and optimal parameters for continuous feedback chaos control

Y. Chembo Kouomou[1,2] and P. Woafo[1,*]
[1]*Laboratoire de Mécanique, Faculté des Sciences, Université de Yaoundé I, Boîte Postal 812, Yaoundé, Cameroun*
[2]*Ecole Nationale Supérieure des Postes et Télécommunications, Yaoundé, Cameroun*

(Received 24 April 2001; revised manuscript received 22 April 2002; published 17 September 2002)

We investigate the conditions under which an optimal continuous feedback control can be achieved. Chaotic oscillations in the single-well Duffing model, with either a positive or a negative nonlinear stiffness term, are tuned to their related Ritz approximation. The Floquet theory enables the stability analysis of the control. Critical values of the feedback control coefficient fulfilling the optimization criteria are derived. The influence of the chosen target orbit, of the feedback coefficient, and of the onset time of control on its duration is discussed. The analytic approach is confirmed by numerical simulations.

DOI: 10.1103/PhysRevE.66.036205 PACS number(s): 05.45.−a

I. INTRODUCTION

Chaotic oscillations are particularly characterized by their unpredictability and high sensitivity to initial conditions. It is therefore easy to understand that they are generally considered as an undesirable phenomenon in engineering, mainly in the cases where high precision or high performance is required. Physiologists have also noticed that brain waves and cardiac pulsations sometimes become chaotic, and wonder if making them periodic may induce important qualitative or quantitative changes in the living beings' vital functions. Recovering a regular dynamics from a chaotic one has been considered in the mathematical and physical communities as a very challenging task, and gave birth to the notion of chaos control with interesting technological and biological applications [1,2].

The interest devoted to that particular problem has led the researchers to develop different techniques [2–6]. Due to its simplicity and the ease to be implemented practically, the continuous chaos controlling method of Pyragas [6] has been applied to control chaos in several physical systems [7,8] and to achieve synchronization of chaotic systems [9,10]. We can mathematically illustrate this approach by the following equation (in vectorial notation):

$$\dot{\mathbf{v}}=\mathbf{f}(\mathbf{v},t)-[\mathbf{K}][\mathbf{v}-\overline{\mathbf{v}}(t)]H(t-T_0), \quad t\geqslant 0, \tag{1}$$

where H is the Heaviside step function defined as

$$H(x)=\begin{cases}0 & \text{if } x<0\\ 1 & \text{if } x\geqslant 0.\end{cases} \tag{2}$$

$\mathbf{K}$ is the feedback gain matrix, $\overline{\mathbf{v}}$ is the target orbit, t is the time, and T_0 is the onset time of the control. Due to the nonlinear vector-flow $\mathbf{f}(\mathbf{v},t)$, the system is assumed to display a chaotic dynamics when $t<T_0$, and for $t\geqslant T_0$, the feedback controllers are supposed to be driving the oscillator from chaos to the desired target orbit.

Solving the retroactive control problem requires the fulfillment of optimization criteria, amongst which the choice of the appropriate target(s) orbit(s), the computation of suitable parameters for the $\mathbf{K}$ matrix, the minimization of the duration of the control. To the best of our knowledge, very few analytical studies have been done in that domain, and the most of the time, the control parameters are chosen on the basis of numerical simulations, or even at random. Therefore, the aim of this paper is, to determine under which conditions the control may be conducted in the most efficient way: that is, in one word, optimization.

For this purpose, we will take one of the most well-known models of nonlinear physics, the single-well Duffing equation, and for simplicity, we will lead the control with a single scalar parameter K according to

$$\ddot{x}+\lambda\dot{x}+x+\gamma x^3=F\cos\omega t-K(x-\overline{x})H(t-T_0), \quad t\geqslant 0. \tag{3}$$

Here, λ is a positive damping coefficient, and γ a nonlinearity coefficient. In fact, Duffing introduced this latter cubic stiffness term in 1918 to describe the hardening ($\gamma>0$) or the softening ($\gamma<0$) spring effects observed in many mechanical problems [11]. We also suppose that the oscillator is excited by an external sinusoidal force of amplitude F and frequency ω, and that the control will be achieved towards the target orbit $(\overline{x},\dot{\overline{x}})$ of the phase plane. This continuous control of chaos by a self-controlling feedback technique has successfully been used both theoretically and experimentally, and its robustness relatively to noise influence has been proved to be effective [6].

The paper is organized as follows. In Sec. II we will approximate the optimal orbits with the Ritz variational criterion in both the $\gamma>0$ and $\gamma<0$ cases. The Floquet theory will enable us to perform the stability analysis of the controlled system in Sec. III; the boundaries of instability domains will be analytically determined. Section IV deals with various considerations such as the existence of a critical value K_{cr} under which no control is possible, the influence of control precision upon this critical value, and the impact of K and T_0 upon the duration T_{con} of the control. Light will also be shed on the variations of T_{con} as a function of the control

*Corresponding author. Email address: pwoafo@uninet.uycdc.cm

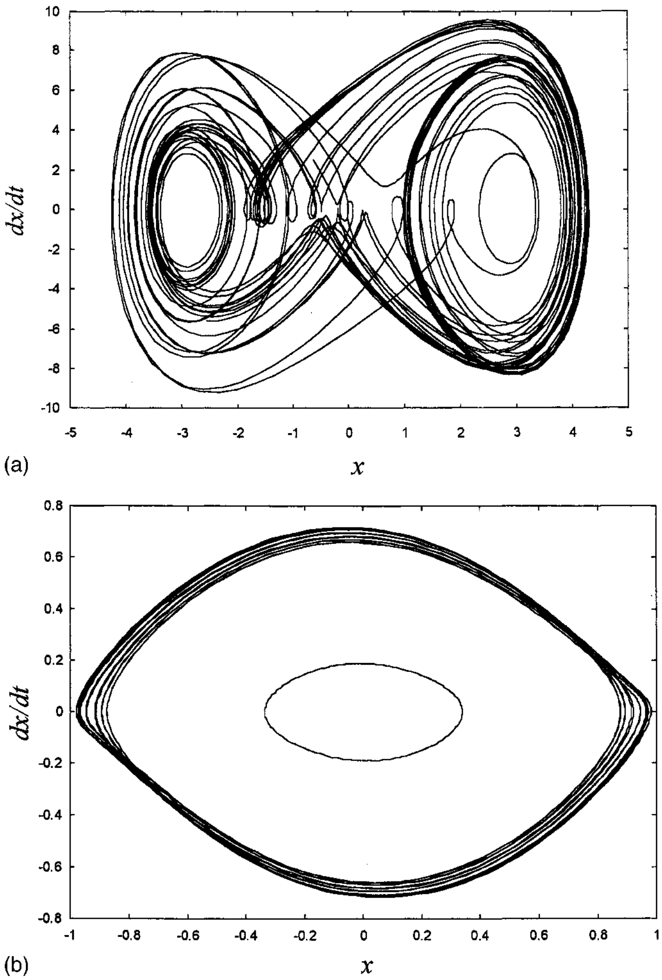

FIG. 1. Phase plane of the chaotic systems. (a) $\gamma>0$ case: $\lambda=0.2$, $\gamma=1.0$, $F=28.5$, and $\omega=0.86$ with initial conditions (0;0). (b) $\gamma<0$ case: $\lambda=0.4$, $\gamma=-1.0$, $F=0.23$, $\omega=0.5255$ with initial conditions (0;0) for the inner limit cycle, and $(-0.3;0.7)$ for the chaotic trajectory.

weight parameter K. We finally conclude in Sec. V. The numerical simulation of all the ordinary differential equations will use the fourth-order Runge-Kutta algorithm, with a time step $h_{\mathrm{RK}}=T/1000$, where $T=2\pi/\omega$ is the period of the external excitation.

II. DETERMINATION AND COMPUTATION OF OPTIMAL TARGET ORBITS

As it is known, the single-well Duffing model can display a chaotic dynamics according to the chosen parameters. In the $\gamma>0$ case [12,13], the system presents the classical jump phenomenon and nonlinear resonance, but high external force amplitudes give rise to chaotic oscillations owing to the pseudo-two-wells potential configuration, as shown in Fig. 1(a). When $\gamma<0$, chaos is much more difficult to spot. For example, the sets of parameters in Fig. 1(b) can induce two different stable orbits depending on initial conditions. We have an inner limit cycle, which has a relatively large basin of attraction including the trivial center point in the phase plane, and an outer chaotic trajectory whose basin of attraction is a thin band separating the inner limit cycle and the unbounded solution basins [14].

It is more advantageous to achieve the control towards a regular orbit which, in the ideal case, satisfies Eq. (3) for $t<T_0$, so that the transition from chaotic to controlled oscillations may be as smooth as possible. Hence, optimization criteria come into play, trying to minimize the function

$$g(t)=F\cos\omega t-(\ddot{\overline{x}}+\lambda\dot{\overline{x}}+\overline{x}+\gamma\overline{x}^3),\quad t\geqslant 0. \tag{4}$$

It has been theoretically demonstrated that the residual function g can uniformly be set equal to zero if the control is conducted towards one of the unstable periodic orbits (UPOs) embedded within the chaotic attractors [3,6]: in that sense, they are the exact optimal target orbits. But generally, these UPOs correspond to nonsinusoidal oscillations, so that it is difficult to define their exact time-dependent analytic expression. Since our objective is to derive the analytical expressions of the chaos control characteristics, we circumvent this problem in the following manner. We approximate the UPOs by regular uniperiodic orbits that nearly satisfy the optimization criterion. Therefore, the approximated minimization of the residue function g can be achieved through several different methods, amongst which we have chosen the Ritz variational criterion, leading to

$$\int_0^{2\pi/\infty} g(t)e^{i\omega t}dt=0. \tag{5}$$

We can take a target orbit of any kind, but for sinusoidal excitations, elliptic trajectories in the phase plane seem to be the most appropriate, and then we set

$$\overline{x(t)}=\overline{x_0}\cos(\omega t-\varphi). \tag{6}$$

Hence, Eq. (5) yields the following set of nonlinear algebraic equations:

$$\left\{\begin{aligned}&\left(\left[1-\omega^2)+\frac{3}{4}\gamma\overline{x}_0^2\right]^2+\lambda^2\omega^2\right]\overline{x}_0^2=F^2,\\ &\varphi=\tan^{-1}\left(\frac{\lambda\omega}{(1-\omega^2)+\frac{3}{4}\gamma\overline{x}_0^2}\right),\end{aligned}\right. \tag{7}$$

and the function g may now be written as

$$g(t)=-\beta\cos(3\omega t-3\varphi), \tag{8}$$

where

$$\beta=\tfrac{1}{4}\gamma\overline{x}_0^3. \tag{9}$$

The Ritz criterion has transformed $g(t)$ into a periodic function whose frequency is thrice that of the external excitation. Equation (7) gives a sixth-order polynom in $\overline{x_0}$, and we have used the Newton-Raphson algorithm to determine its real positive solutions. For the system parameters of Fig. 1(a), we have a single solution

$$\overline{x_{01}}=3.327\,32,\quad \varphi_1=0.020\,08 \tag{10}$$

and for those of Fig. 1(b), we have three, which are

$$\begin{cases} \overline{x_{01}}=0.343\,74, & \varphi_1=0.319\,56 \\ \overline{x_{02}}=0.864\,79, & \varphi_2=0.911\,34 \\ \overline{x_{03}}=1.031\,61, & \varphi_3=-1.230\,96 \end{cases} \tag{11}$$

with a 10^{-5} precision. For the $\gamma<0$ case, the first inner Ritz orbit can straightforwardly be identified to the stable periodic orbit of the uncontrolled system, while the second Ritz orbit, which is always unstable according to the classical nonlinear analysis (hysteresis), constitutes a fairly good approximation of the UPO embedded within the chaotic attractor. For the $\gamma>0$ case, the approximation is certainly less pertinent because the Ritz variational approximation is poor as the UPOs in this case are more complicated.

Nevertheless, the Ritz procedure has the advantage to provide sets of purely sinusoidal target variables to the feedback controller, according to what is the most prevalent scheme in practice. These approximated optimal orbits can also serve as interesting alternatives when time-delayed [6] or computer-assisted [3] controllers are unavailable or inappropriate, hence keeping the exact UPOs out of reach. Moreover, their explicit time-dependent expression would probably enable one to perform a stability analysis valid for the neighboring case of the true optimal orbits, i.e., UPOs. That is why, in all subsequent sections, we will rather tune the chaotic oscillations to their related regular Ritz orbits. Note that throughout the paper, the $\gamma>0$ and $\gamma<0$ cases will refer to the sets of parameters used, respectively, in Figs. 1(a) and 1(b).

III. STABILITY ANALYSIS OF THE CONTROL

Starting from $t=T_0$, the system changes its configuration, and stability considerations come into play. Quite few studies have been done on that topic despite its crucial importance. We emphasize that stability is not control, because the notion of control implies the $\mathrm{Sup}(x-\overline{x})\leqslant h$ condition, h being the precision of the control, while stability, which is less restrictive, just requires x to remain bounded. Therefore, one can tolerate the control to fail $[\mathrm{Sup}(x-\overline{x})>h]$, but never to be unstable, since it would cause irreversible damages to the system.

The stability of the control is strictly equivalent to the boundedness of ε defined as

$$\varepsilon(t)=x(t)-\overline{x}(t), \quad t\geqslant T_0. \tag{12}$$

Here, we have introduced a new variable which is the measure of the relative nearness of both controlled and target orbits. From Eq. (3), one can therefore deduce that, for $t\geqslant T_0$, ε obeys

$$\ddot{\varepsilon}+\lambda\dot{\varepsilon}+[\Omega_0^2+\eta\cos(2\omega t-2\varphi)]\varepsilon+\mu\varepsilon^2\cos(\omega t-\varphi)+\gamma\varepsilon^3 = -\beta\cos(3\omega t-3\varphi) \tag{13a}$$

with

$$\Omega_0^2=1+K+\tfrac{3}{2}\gamma\overline{x_0^2}, \tag{13b}$$

$$\eta=\tfrac{3}{2}\gamma\overline{x_0^2},$$

$$\mu=3\gamma\overline{x_0},$$

$\overline{x_0}$ and φ being the coefficients of the Ritz solution. Equation (13a), which is nonlinear with an excitation both parametric and external, can be unstable for certain values of K, i.e., lead to unbounded solutions. Effectively, if we only keep linear terms in ε (since ε is assumed to be small), and discard the external excitation (which does not induce unstable oscillations at that approximation), the boundedness of ε would be established by the study of the linear parametric equation

$$\ddot{\varepsilon}+\lambda\dot{\varepsilon}+[\Omega_0^2+\eta\cos(2\omega t-2\varphi)]\varepsilon=0, \tag{14}$$

which is a damped version of the Mathieu equation. Equation (14) presents instability domains according to λ, Ω_0, ω, and η. The Floquet theory tackles this problem by precising the stability boundaries [15–17]. By setting the following rescalings,

$$\tau=\omega t, \qquad u(\tau)=\varepsilon\exp\left(\frac{\lambda\tau}{2\omega}\right), \tag{15}$$

the dissipative Mathieu equation can be rewritten in the canonical form as

$$\ddot{u}+[\delta+2\alpha\cos(2\tau-2\varphi)]u=0 \tag{16}$$

with

$$\delta=\frac{1}{\omega^2}\left[\Omega_0^2-\frac{\lambda^2}{4}\right]=\frac{1}{\omega^2}\left[1+K+\frac{3}{2}\gamma\overline{x_0^2}-\frac{\lambda^2}{4}\right],$$

$$\alpha=\frac{\eta}{2\omega^2}=\frac{3\gamma\overline{x_0^2}}{4\omega^2}. \tag{17}$$

Hence, the control parameter K only modifies δ, but not α anyway. The solution of Eq. (16) has the form

$$u(\tau)e^{\theta\tau}\phi(\tau), \tag{18}$$

where ϕ is a π-periodic function and θ a complex number. Expanding ϕ in Fourier series yields

$$\phi(\tau)=\sum_{n=-\infty}^{+\infty}\phi_n e^{2in\tau} \tag{19}$$

and hence

$$u(\tau)=e^{\theta\tau}\phi(\tau)=\sum_{n=-\infty}^{+\infty}\phi_n e^{(\theta+2in)\tau}. \tag{20}$$

Inserting Eq. (20) in Eq. (16) gives an infinite homogeneous, linear, and algebraic system, which may have solutions if and only if the associated determinant is set equal to zero, that is

$$\Delta(\theta)=\left\|\frac{(\delta+(\theta+2im)^2)\delta_{m,n}+\alpha(e^{2i\varphi}\delta_{m,n-1}+e^{-2i\varphi}\delta_{m,n+1})}{\delta-(2m)^2}\right\|=0, \tag{21}$$

where the $\delta_{m,n}$ are Kronecker symbols [17]. The determinant of Eq. (21) is called the infinite Hill determinant, and one can show that it obeys

$$\Delta(\theta)=\Delta(0)-\frac{\sin^2(\frac{1}{2}i\pi\theta)}{\sin^2(\frac{1}{2}\pi\sqrt{\delta})} \tag{22a}$$

and therefore

$$\theta=\pm\frac{2i}{\pi}\sin^{-1}\sqrt{\Delta(0)\sin^2(\tfrac{1}{2}\pi\sqrt{\delta})}. \tag{22b}$$

Since, from Eqs. (15),

$$\varepsilon(\tau)=\phi(\tau)\exp\left[\left(\theta-\frac{\lambda}{2\omega}\right)\tau\right], \tag{23}$$

we can deduce, depending on the real part of θ, that the ε oscillations either decay to zero or continuously increase to infinity, unless $\mathrm{Re}(\theta)=\lambda/2\omega$. Floquet theory states that the transition from stability to instability occurs only in two distinct conditions.

(1) π-periodic transition: $\theta=\lambda/2\omega$.

$$\Delta(0)+\frac{\sinh^2\left(\frac{\lambda\pi}{4\omega}\right)}{\sin^2(\frac{1}{2}\pi\sqrt{\delta})}=0. \tag{24}$$

(2) 2π-periodic transition: $\theta=i+\lambda/2\omega$.

$$\Delta(0)-\frac{\cosh^2\left(\frac{\lambda\pi}{4\omega}\right)}{\sin^2(\frac{1}{2}\pi\sqrt{\delta})}=0. \tag{25}$$

Equations (24) and (25) define a set of curves in the (δ,α) plane, as approximately represented in Fig. 2 (for exact curves, see Refs. [15–17]). For the nondissipative Mathieu equation, the Hopf theorem states that for a fixed α, stable values of δ are those which are strictly situated between boundaries of different types. In our dissipative case, it graphically implies that the stability domain is the shaded area of Fig. 2. Mathematically, if we define the new real function

$$\Gamma(\delta,\alpha)=\begin{cases}\Delta(0)\sin^2\left(\frac{1}{2}\pi\sqrt{\delta}\right) & \text{if } \delta\geqslant 0\\ -\Delta(0)\sinh^2\left(\frac{1}{2}\pi\sqrt{-\delta}\right) & \text{if } \delta<0.\end{cases} \tag{26}$$

The Hopf theorem leads to the following stability condition:

$$-\sinh^2\left(\frac{\lambda\pi}{4\omega}\right)<\Gamma(\delta,\alpha)<+\cosh^2\left(\frac{\lambda\pi}{4\omega}\right). \tag{27}$$

We have earlier noticed that the control parameter K only modifies δ, but not α. Hence, when K is varied, the figurative of the system in the (δ,α) plane is just moving along a $\alpha=\text{const}$ straight horizontal line. Starting from $\delta=-\infty$ [i.e., $K=-\infty$ according to Eq. (17)], this point will alternatively pass through unstable and stable domains. Hence, as far as stability is concerned, a proper choice of K requires the fulfillment of the double inequality (27).

Qualitatively, numerical simulations fully agree with the above analytic statements. The unique solution of the $\gamma>0$ case generates a high α value: hence, we have several stability intervals of the kind $]K_{b1},K_{b2}[$, $]K_{b3},K_{b4}[,\ldots,$ $]K_{bn},+\infty[$, where the K_{bi} are boundary values for K. Since $\overline{x_0}$ is large, the nonlinear terms of Eq. (13a) play a predominant stabilizing role, and gather all the compact intervals $]K_{bi},K_{b(i+1)}[$ within $]-17.5,-17.4[$. If we notice that $\delta=0$ corresponds here to $K_0=-17.560$, we can deduce that the system surprisingly behaves as if α was very small, possessing a single stability interval $]K_0,+\infty[$ at the first approximation. The two solutions of the $\gamma<0$ case generate a lower α, (in absolute value) and then, lead to just two stability intervals of the form $]K_{b1},K_{b2}[$ and $]K_{b3},+\infty[$: numerically, we have for the first solution ($K_{b1}=-0.434$; $K_{b2}=0.017$; $K_{b3}=1.228$) and for the second ($K_{b1}=-0.231$; $K_{b2}=0.008$; $K_{b3}=2.762$). These intervals correspond to the two segments laying within the shaded area in Fig. 2. Obviously, $K=0$ (corresponding to a no-control situation) always belongs to a stability interval. In fact, it was *a priori* evident that negative values are not, in general, appropriate for the control, contrary to what occurs in synchronization theory

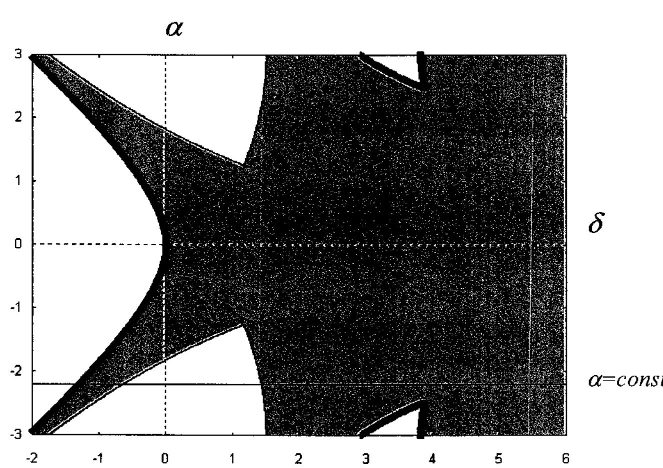

FIG. 2. Stability diagram in the (δ,α) plane showing the π-periodic boundaries (thick lines) and 2π-periodic boundaries (thin lines).

[18]. But the Floquet theory enables us to point out a quite interesting conclusion, confirmed by numerical simulations: even small positive values of K can destabilize a system, while higher values scarcely do.

It should be noticed that the control towards UPOs nearly correspond to the case $\beta=0$ (i.e., $g\equiv 0$). Since β has no influence on the linear stability pattern, one can expect that the conclusions derived for the Ritz orbits are qualitatively valid for the exact optimal orbits. Anyway, the accuracy of the stability analysis can be sharpened by the expansion of the approximation to the harmonics of ω (mainly for the $\gamma>0$ case).

IV. CRITICAL PARAMETERS AND DURATION OF CONTROL

As we have earlier noticed, stability is not control: appropriate values for K are those for which

$$|\varepsilon(t)|<h, \quad t>(T_0+T_{\mathrm{con}}), \tag{28}$$

where h is the precision of the control, and T_{con} its duration, that is, the interval between the onset time of the control and the time of its end. The stability analysis suggests that very large values of K are always good, but it would be very interesting to determine the critical value K_{cr} under which, for a given precision, no control is possible. The advantage of such an investigation is at least twofold: first, it enables one to ensure the control with the smallest K possible, which is equivalent to the lowest energy input; second it permits one to know how the parameters of the system affect this critical value.

When K is varied, Ω_0 is modified according to Eqs. (13), and since ω is a fixed frequency, resonances may occur with the external and parametric excitations. The method of multiple time scales demonstrates that the last peak of resonance is induced by the external excitation: hence, Ω_0 should be far beyond 3ω if we want to obtain small amplitudes for ε. We can therefore neglect the nonlinear terms (because of the small amplitudes of ε, precisely), and discard the linear parametric excitation (which does not induce noticeable resonance), and obtain the following simplified version of Eq. (13a):

$$\ddot{\varepsilon}+\lambda\dot{\varepsilon}+\Omega_0^2\varepsilon=-\beta\cos(3\omega t-3\varphi), \quad t\geqslant T_0. \tag{29}$$

The control is ensured when the precision h is greater than the amplitude of the ε steady-state oscillations. The critical value of K above which it is the case is precisely obtained by setting the equality between the both, yielding

$$K_{\mathrm{cr}}=9\omega^2-1-\frac{3}{2}\gamma\overline{x}_0^2+\sqrt{\left(\frac{\gamma\overline{x}_0^3}{4h}\right)^2-9\lambda^2\omega^2} \tag{30}$$

assuming that

$$h<\frac{|\gamma|\overline{x}_0^3}{12\lambda\omega}. \tag{31}$$

Figures 3(a) and 3(b) show the quasiperfect coincidence between formula (30) and the results of the numerical simulation of the differential equation (3), and therefore confirm its validity. It obviously appears that K_{cr} is a decreasing function of the precision h. Sometimes, the Routh-Hurwitz criterion is used to determine K_{cr} [7,8], but it unfortunately fails to include the influence of the precision, and then to fulfill accuracy requirements. For the $\gamma>0$ case, one can notice in Fig. 3(a) that very large K are necessary to ensure the control, even for poor precisions: this is due to the large amplitude $\overline{x_0}$ of the target motion. For the $\gamma<0$ case, Fig. 3(b) confirms that higher K are required for large $\overline{x_0}$. This latter case is interesting since it enables a quantitative comparison between orbits of the same system's parameters: it is noticeable that the control is more difficult to achieve with the second orbit, that is near the chaotic band than with the first which is far away. Another marginal phenomenon can be reported. Control towards the first solution in the $\gamma<0$ case also occurs when K belongs to the intervals $]-0.434, -0.036[$ and $]0.001,0.017[$, which almost correspond to the whole first stability interval: this apparently violates condition (30). In fact, the retroactive feedback term $-K(x-\overline{x})$ acts in that case as a small perturbation of the sensitive

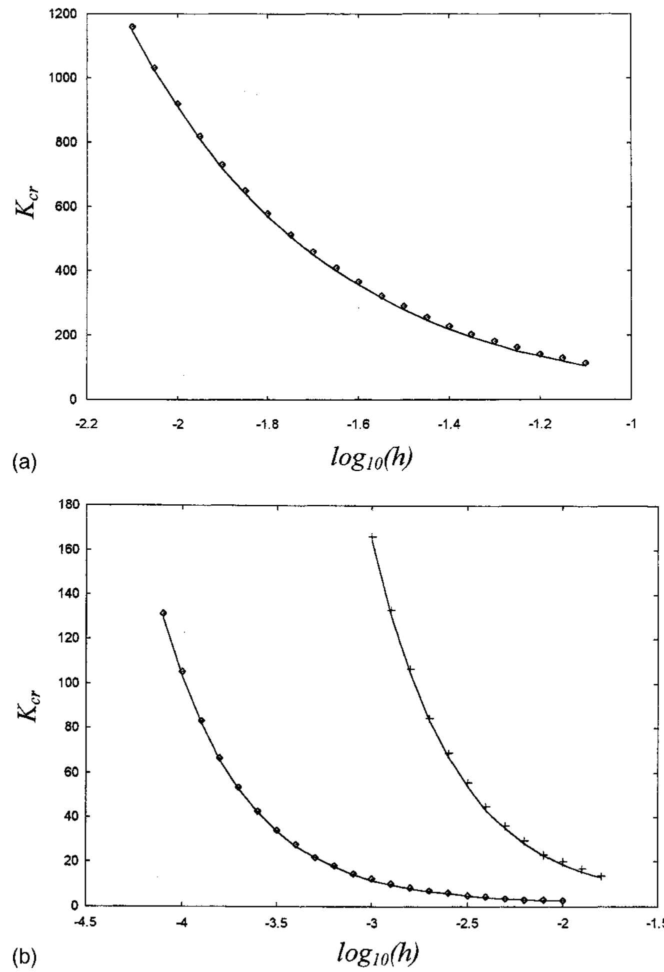

FIG. 3. K_{cr} as a function of $\log_{10}(h)$ (full lines for analytic results, squares and crosses for numerical results). (a) $\gamma>0$ case. (b) $\gamma<0$ case with the lower curve for the first solution and the upper one for the second.

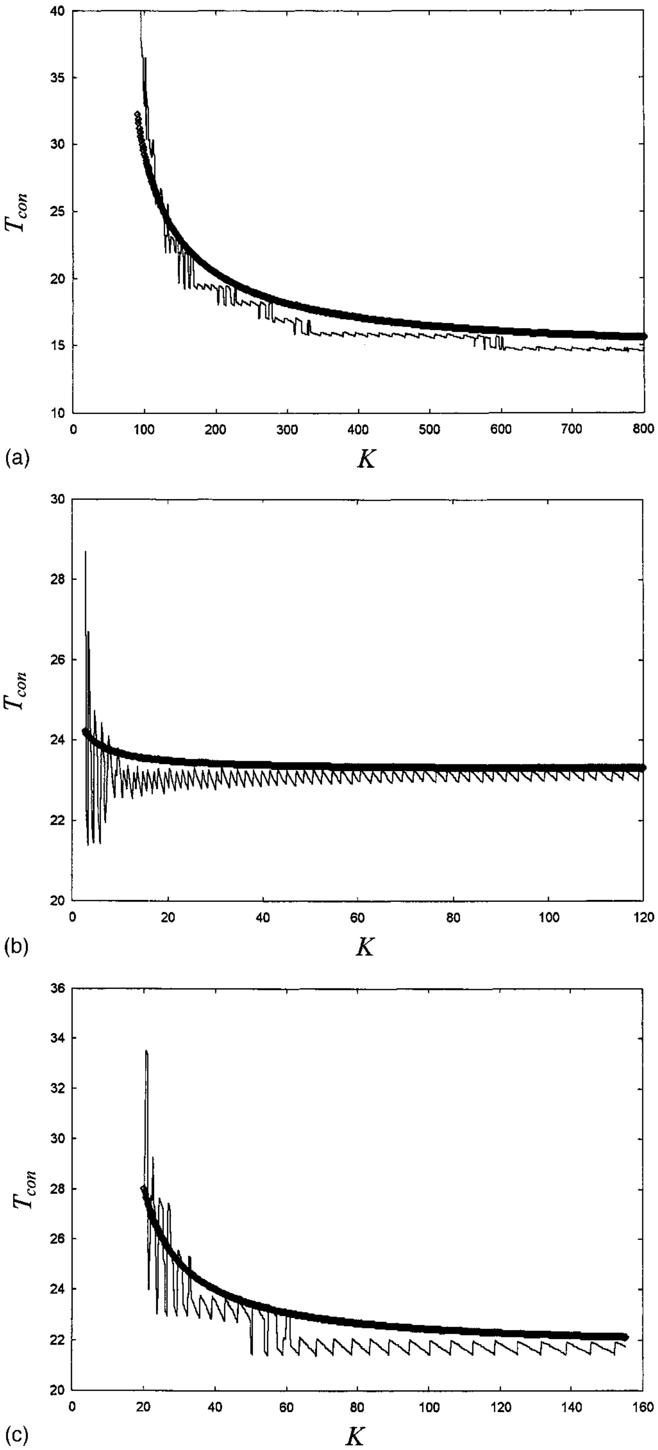

FIG. 4. T_{con} as a function of K (thick lines for analytic results, and thin lines for numerical results). (a) $\gamma>0$ case with $T_0=100$ and $h=10^{-1}$; (b) $\gamma<0$ case, first solution with $T_0=100$ and $h=10^{-2}$; (c) $\gamma<0$ case, second solution with $T_0=100$ and $h=10^{-2}$.

chaotic orbit, which then degenerates into the inner limit cycle. Therefore this scheme may be interpreted as a jump phenomenon, rather than a control process.

It appears that the control towards the Ritz orbits requires a defined minimal input energy. This can be explained by the fact that they are not dynamically intrinsic solutions of the uncontrolled Duffing system. For UPOs, the residual function g vanishes and the ε variable is no more externally excited: therefore, to foresee the success of the control procedure, the determination of the θ exponent [which passes through the computation of the infinite Hill determinant $\Delta(0)$] would be necessary.

Equation (29) can also be used to derive explicitly the duration of the control, which can be assimilated to the time required for the transient oscillations to decay, that is,

$$T_{\mathrm{con}}=\frac{2}{\lambda}\ln\left[\frac{\sqrt{\dot{\varepsilon}^2(T_0)+\dfrac{[\dot{\varepsilon}(T_0)+\lambda\varepsilon(T_0)/2]^2}{\Omega_0^2-\lambda^2/4}}}{h-\dfrac{|\beta|}{\sqrt{(\Omega_0^2-9\omega^2)^2+9\lambda^2\omega^2}}}\right]. \quad (32)$$

T_0 implicitly influences T_{con} through $\varepsilon(T_0)$, since the duration of the control logarithmically increases with the initial separation between the chaotic and the target orbits in the phase plane. Hence, one should note that T_{con} can be very low only when the target orbit is near the chaotic trajectory (even though, as we have earlier demonstrated, the control paradoxically requires more energy in that case). On the other hand, as numerically confirmed by Fig. 4, T_{con} is a decreasing function of K, and one can find that

$$T_{\mathrm{con,min}}=\lim_{K\to+\infty}T_{\mathrm{con}}=\frac{2}{\lambda}\ln\left[\frac{|\varepsilon(T_0)|}{h}\right] \quad (33)$$

is the minimum duration under which no control can be achieved. This result is of great practical interest. *A priori*, one could have naively thought that the control could have been led as fast as desired, just depending on K: Figure 4 does not support that. For example, Fig. 4(b) shows that a feedback coefficient $K=10$ is sufficient to ensure an optimal control (with approximately the minimum T_{con}). Hence, the above analysis enables us to avoid an unavailing waste of input energy by preventing us from a useless increase of the control parameter K. Anyway, the interest of all the above statements is unfortunately limited by the fact that $\varepsilon(T_0)=x(T_0)-\overline{x(T_0)}$ is always an unknown because of $x(T_0)$. Nevertheless, it is possible to perform an analysis leading to statistical conclusions.

One may wonder why the curves of Fig. 4 obtained through the numerical simulation of Eq. (3) are not smooth. We need to refer again to the Floquet theory to explain that phenomenon. It should first be noticed that K_{cr} always belongs here to the last stability domain: it implies that all the values beyond K_{cr} are at least stable. The θ exponent, whose real part permits one to determine the decay rate according to Eq. (23) is explicitly defined as follows:

$$-\sinh^2\left(\frac{\lambda\pi}{4\omega}\right)<\Gamma\leqslant 0,\quad \theta=\pm 2i\pm\frac{2}{\pi}\sinh^{-1}\sqrt{-\Gamma}, \quad (34)$$

$$0<\Gamma<1,\quad \theta=\pm\frac{2i}{\pi}\sin^{-1}\sqrt{\Gamma},$$

$$1\leqslant\Gamma<\cosh^2\left(\frac{\lambda\pi}{4\omega}\right),\quad \theta=\pm i\pm\frac{2}{\pi}\cosh^{-1}\sqrt{+\Gamma}.$$

It can therefore be deduced that the associated durations of control may, respectively, be derived as

$$-\sinh^2\left(\frac{\lambda\pi}{4\omega}\right)<\Gamma\leqslant 0,\quad \tilde{T}_{\rm con}=T_{\rm con}\frac{1}{1-\dfrac{4\omega}{\lambda\pi}\sinh^{-1}\sqrt{-\Gamma}},$$

$$0<\Gamma<1,\quad \tilde{T}_{\rm con}=T_{\rm con},\tag{35}$$

$$1\leqslant\Gamma<\cosh^2\left(\frac{\lambda\pi}{4\omega}\right),\quad \tilde{T}_{\rm con}=T_{\rm con}\frac{1}{1-\dfrac{4\omega}{\lambda\pi}\cosh^{-1}\sqrt{+\Gamma}},$$

where $\tilde{T}_{\rm con}$ is the new duration of control, and $T_{\rm con}$ is the former one defined by Eq. (32). Hence, as K is increasing, $\Gamma(\delta,\alpha)$ is varying and induces a modulation of $T_{\rm con}$ mainly when $\Gamma(\delta,\alpha)$ is not between 0 and 1. Such variations are also encountered in synchronization theory, even though they are quite larger [10].

Deeper investigations can even permit to foresee the position of the peaks of these curves, that is, the K values for which $\tilde{T}_{\rm con}$ presents a local maximum. Effectively, the Floquet theory demonstrates that at the first approximation, parametric resonance in the Mathieu equation arises when

$$\delta=n^2,\tag{36}$$

n being a positive integer. According to Eq. (17), the corresponding values for K are

$$K_n=n^2\omega^2-\left(1+\frac{3}{2}\gamma\overline{x}_0^2-\frac{\lambda^2}{4}\right).\tag{37}$$

Once again, numerical simulation confirms this deduction. For example, if we consider the control towards the first solution of the $\gamma<0$ case [Fig. 4(b)], we have $K_{\rm cr}=2.458$ (which is above $K_3=1.702$) and analytic maxima given by Eq. (37) are $K_4=3.635$ [numerically, Fig. 4(b) gives 3.623], $K_5=6.120$ (numerically, 6.113), $K_6=9.158$ (9.156), $K_7=12.748$ (12.758), $K_8=16.890$ (16.881), $K_9=21.585$, (21.601), and so on. It is quite remarkable that integer values come into play for the determination of these maxima, even though we are achieving a continuous control. Nevertheless, it is important to note that other peaks may appear, because of the parametric and nonlinear resonances we have neglected. Anyway, these K_n values obviously lead to a slower control, and the above analysis at least enables one to avoid them.

V. CONCLUSION

In summary, we have investigated the conditions under which an optimal continuous feedback control can be led. The example of the generalized single-well Duffing model has enabled us to understand the occurrence of stability intervals according to the control weight parameter. We have also discussed the influence of the precision and of the system's parameters upon the critical feedback coefficient $K_{\rm cr}$ and the duration of the control.

Perspectives for such a work are numerous. The first step is to generalize the strategy we have developed to multidimensional coupled systems, and to other types of target orbits. Other subjective optimization criteria can also be adopted. For instance, in wire telecommunication systems, the feedback term can correspond to an undesirable crosstalk phenomenon: in this case, the goal to reach is to keep K as low as possible, and then, $K_{\rm cr}$ will here rather be a maximum above which, for a given precision, the signals x (useful) and $\overline{x}$ (parasite) may unfortunately not be considered as independent anymore. The study can also be extended to the synchronization of chaotic oscillators: the matter would therefore be to find the K values for which negative sub-Lyapunov exponents are obtained.

[1] A. Garfinkel, M. L. Spano, W. L. Ditto, and J. N. Weiss, Science **257**, 1230 (1992); V. Petrov, V. Gaspar, J. Masere, and K. Showalter, Nature (London) **361**, 240 (1993); S. J. Schiff, K. Jerger, D. H. Duong, T. Chang, K. L. Spano, and W. L. Ditto, *ibid.* **370**, 615 (1994); K. Hall, D. J. Christini, M. Tremblay, J. J. Collins, L. Glass, and J. Billette, Phys. Rev. Lett. **78**, 4518 (1997).

[2] T. Kapitaniak, *Controlling Chaos* (Academic, London, 1996); M. Lakshamanan and K. Murali, *Chaos in Nonlinear Oscillators, Controlling and Synchronization* (World Scientific, Singapore, 1996).

[3] E. Ott, C. Grebogi, and Y. A. Yorke, Phys. Rev. Lett. **64**, 1196 (1990).

[4] W. L. Ditto, S. N. Rauseo, and M. L. Spano, Phys. Rev. Lett. **65**, 3211 (1990).

[5] T. Shinbrot, E. Ott, C. Grebogi, and Y. A. Yorke, Phys. Rev. Lett. **65**, 3215 (1990).

[6] K. Pyragas, Phys. Lett. A **170**, 421 (1992).

[7] G. Chen and X. Dong, IEEE Trans. Circuits Syst., I: Fundam. Theory Appl. **40**, 591 (1993).

[8] Y. Chembo Kouomou and P. Woafo, Phys. Scr. **62**, 255 (2000).

[9] T. Kapitaniak, Phys. Rev. E **50**, 1642 (1994).

[10] P. Woafo, Phys. Lett. A **267**, 31 (2000).

[11] G. Duffing, *Erzwungene Schwingungen bei Veränderlicher Eigenfrequenz* (F. Vieweg u Sohn, Braunschweig, Germany, 1918).

[12] C. Pezeschki and E. H. Dowell, Physica D **32**, 194 (1988).

[13] U. Parlitz and W. Lauterborn, Phys. Lett. **107A**, 351 (1985).

[14] A. H.-D. Cheng, C. Y. Yang, K. Hackl, and M. J. Chajes, Int. J. Non-Linear Mech. **28**, 549 (1993).

[15] J. J. Stocker, *Nonlinear Vibrations in Mechanical and Electrical Systems* (Interscience, New York, 1950).

[16] C. Hayashi, *Nonlinear Oscillations in Physical Systems* (McGraw-Hill, New York, 1964).

[17] A. H. Nayfeh and D. T. Mook, *Nonlinear Oscillations* (Wiley, New York, 1979).

[18] K. Leung, Phys. Rev. E **58**, 5704 (1998).